Published in final edited form as:
Neuron. 2006 January 19; 49(2): 229–241. doi:10.1016/j.neuron.2005.12.011.

Calnexin Is Essential for Rhodopsin Maturation, Ca^{2+} Regulation, and Photoreceptor Cell Survival

Erica E. Rosenbaum[1], **Roger C. Hardie**[2], and **Nansi J. Colley**[1,*]

[1]Department of Ophthalmology and Visual Sciences and Department of Genetics University of Wisconsin Madison, Wisconsin 53792

[2]Department of Anatomy Cambridge University Downing Street Cambridge CB2 3DY United Kingdom

Summary

In sensory neurons, successful maturation of signaling molecules and regulation of Ca^{2+} are essential for cell function and survival. Here, we demonstrate a multifunctional role for calnexin as both a molecular chaperone uniquely required for rhodopsin maturation and a regulator of Ca^{2+} that enters photoreceptor cells during light stimulation. Mutations in *Drosophila calnexin* lead to severe defects in rhodopsin (Rh1) expression, whereas other photoreceptor cell proteins are expressed normally. Mutations in *calnexin* also impair the ability of photoreceptor cells to control cytosolic Ca^{2+} levels following activation of the light-sensitive TRP channels. Finally, mutations in *calnexin* lead to retinal degeneration that is enhanced by light, suggesting that calnexin's function as a Ca^{2+} buffer is important for photoreceptor cell survival. Our results illustrate a critical role for calnexin in Rh1 maturation and Ca^{2+} regulation and provide genetic evidence that defects in *calnexin* lead to retinal degeneration.

Introduction

G protein-coupled receptors are synthesized on membrane-bound ribosomes and undergo translocation, modification, folding, oligomeric assembly, and quality control in the endoplasmic reticulum (ER) (Ellgaard and Helenius, 2003b). To deal with these complex and error-prone processes, the ER has evolved a system centered around the calnexin family of molecular chaperones, which promotes the proper folding and assembly of newly synthesized glycoproteins. Calnexin is a type I transmembrane protein that, like its soluble ER homolog calreticulin, interacts with the monoglucosylated glycan ($Glc_1Man_{7–9}GlcNAc_2$) present on folding intermediates of glycoproteins. Nascent glycoproteins associate with calnexin or calreticulin via a cycle of binding and release. (Ellgaard and Helenius, 2003a; Molinari et al., 2004; Schrag et al., 2001; Ware et al., 1995). This cycle is key for ER quality control, as it inhibits aggregation, prevents premature exit from the ER, and exposes glycoproteins to accessory enzymes and folding factors (Ellgaard and Helenius, 2003a). Despite considerable understanding of the calnexin/calreticulin cycle, little is known about the requirement for calnexin in protein processing in vivo.

Rhodopsin is the prototypical member of the vast G protein-coupled receptor family. As in vertebrates, *Drosophila* rhodopsin (Rh1) initiates the phototransduction cascade by

*Correspondence: njcolley@wisc.edu.

Supplemental Data
The Supplemental Data for this article can be found online at http://www.neuron.org/cgi/content/full/49/2/229/DC1/.

interacting with a heterotrimeric G protein, which then activates a distinct effector enzyme, namely phospholipase C (PLC-β). Activation of PLC leads to the opening of the cation-selective TRP and TRPL channels, resulting in a dramatic rise in intracellular Ca^{2+} (reviewed in Hardie and Raghu, 2001; Pak and Leung, 2003).

To become functionally active, newly synthesized rhodospin must be precisely folded and successfully navigate the secretory pathway to the phototransducing compartment of the photoreceptor cells, the rhabdomeres (Colley et al., 1991). Rhabdomeres consist of numerous tightly packed microvilli containing the phototransduction machinery. The mechanisms that regulate the folding and transport of rhodopsin are essential for photoreceptor cell function and survival, as defects in rhodopsin maturation lead to retinal degeneration in both *Drosophila* and vertebrates (Colley et al., 1991, 1995; Kurada and O'Tousa, 1995; Pacione et al., 2003; Sung and Tai, 2000; Webel et al., 2000). Protein maturation defects characterized in blinding diseases have broad implications, as protein misfolding and aggregation are characteristic of a variety of neurodegenerative diseases, including Alzheimer's disease, Parkinson's disease, and Huntington's disease (Muchowski and Wacker, 2005). Here, we investigate whether calnexin functions as a chaperone for Rh1 and whether mutations in *calnexin* lead to neurodegeneration.

In addition to its role as a molecular chaperone, calnexin is thought to bind Ca^{2+} at two distinct sites. The first resides in the long N-terminal domain localized to the lumen of the ER. The crystal structure of vertebrate calnexin shows that this luminal domain consists of two distinct regions: a compact, globular domain and a proline-rich arm called the P domain (Figure 1A). The globular domain is thought to bind a single Ca^{2+} ion and is also involved in glucose binding (lectin domain) (Schrag et al., 2001). Although less well defined, several lines of evidence suggest that calnexin may harbor a second Ca^{2+}-binding domain within the highly charged C-terminal cytosolic tail (C domain). Interestingly, this cytosolic domain displays structural similarity to calreti-culin's luminal C domain, but is positioned on the opposite, cytosolic side of the ER membrane (Tjoelker et al., 1994). Calreticulin's C domain displays low-affinity and high-capacity Ca^{2+} binding and is thought to buffer luminal Ca^{2+} (Baksh and Michalak, 1991). While the in vivo role of calnexin's C domain is unknown, these Ca^{2+}-binding properties would make it ideal for buffering high concentrations of cytosolic Ca^{2+}.

Precise spatial and temporal control over Ca^{2+} levels is essential for phototransduction in both vertebrates and invertebrates. Furthermore, prolonged elevation of cytosolic Ca^{2+} can be toxic, leading to cell death (Dolph et al., 1993; Fain and Lisman, 1999; Wang et al., 2005). In *Drosophila*, the light-sensitive TRP and TRPL channels mediate a massive Ca^{2+} influx into the rhabdomeres that is essential for amplification, rapid-response kinetics, and light adaptation (Hardie and Raghu, 2001). Ca^{2+} can rise to about 1 mM in the rhabdomeres (Postma et al., 1999) and is removed from the rhabdomeres by a combination of the Na^{+}/Ca^{2+} exchanger (CalX) (Oberwinkler and Stavenga, 2000; Wang et al., 2005) and diffusion into the cell body, where Ca^{2+} rises to about 10 μM. The mechanisms controlling Ca^{2+} in the cell body are poorly understood but presumably include sequestration by the sarco-endoplasmic reticulum Ca^{2+} ATPase (SERCA) (Hardie, 1996a) and buffering by cytosolic Ca^{2+}-binding proteins. Here, we explore the hypothesis that calnexin serves as a buffer for cytosolic Ca^{2+} following the acute Ca^{2+} rise during phototransduction and that it may thereby help to prevent Ca^{2+} toxicity and promote photoreceptor cell survival.

In this report, we demonstrate a multifunctional role for calnexin as both a critical molecular chaperone for Rh1 biosynthesis and a regulator of cytosolic Ca^{2+}. Mutations in *calnexin* cause retinal degeneration that is enhanced by light, suggesting that calnexin's role in Ca^{2+} removal may be important for photoreceptor cell survival. These results provide genetic

evidence that failure in Rh1 maturation and Ca^{2+} overload, resulting from defects in calnexin, are responsible for retinal degeneration.

Results

Mutations in *Drosophila calnexin*

By screening the Zuker collection of EMS-mutagenized *Drosophila* lines, we identified two independent mutants that displayed a severe reduction in Rh1 compared to wild-type (wt) (Figure 2A, lanes 1–3). We established that the two mutants were allelic, as the transheterozygotes displayed reduced levels of Rh1 (Figure 2A, lane 4). Furthermore, we established that both alleles were recessive (Figure 2A, lanes 8 and 9).

To identify the mutant locus responsible for the phenotype, we first used deficiency mapping to narrow the cytogenetic location to 99A7 on the third chromosome, corresponding to four genes (Figure 1C and Figure 2A, lanes 5 and 6). We sequenced this small region and identified mutations in the coding region of *calnexin* in both alleles (Brody et al., 2002; Christodoulou et al., 1997). We found that one allele harbored a C to T transition at nucleotide position 544, causing a premature stop codon at glutamine182, and that the other allele harbored a G to A transition at nucleotide position 356, causing a premature stop codon at tryptophan119. Based on cytology, we designated the two alleles *cnx99A*^{1} (*cnx*^{1}) and *cnx99A*^{2} (*cnx*^{2}), respectively. *Drosophila* calnexin99A (Cnx) displays 49% amino acid identity with human calnexin (chromosome 5q), shown in Figure 1B.

To provide further evidence that mutations in *cnx* were responsible for the severe reduction in Rh1, we introduced the wt *cnx* gene into the *cnx* mutants by using a duplication for 99A that was translocated to the X chromosome [Dp(3;1) B152] and confirmed that it restored the normal function (Figures 1C and 2A, lane 7). Consistent with the presence of the stop codons, the *cnx* mutants displayed severely reduced levels of *cnx* transcript (Figure 2B, lanes 1, 2, 5, and 6). In addition, the Cnx protein was absent in both of the *cnx* mutants (Figure 2C, lanes 2 and 3), while it was detected in wt flies (Figure 2C, lane 1). Lane 4 confirms that the mutants were allelic. Cnx protein was not detected in the *cnx*^{1} and *cnx*^{2} mutants when they were crossed to a deficiency (Df) that eliminated 99A (Df(3R)Ptp99A[R3]) (Figure 2C, lanes 5 and 6). These data supported the hypothesis that the mutations were in the *cnx* gene.

Calnexin is thought to play a role in the folding of a large number of proteins. Consistent with this notion, *cnx* was ubiquitously expressed at all stages during development and in the adult (Figure 2B). *cnx* transcript was detected in wt embryos (Figure 2B, lane 9), larvae (Figure 2B, lane 8), and adult heads and bodies (Figure 2B, lanes 3 and 7, respectively). *cnx* transcript and Cnx protein were also detected in heads from flies lacking eyes (*eya*^{1}) (Figure 2B, lane 4, and Figure 2C, lane 8), indicating that *cnx* expression was not restricted to the eyes. Despite the widespread expression pattern of *cnx*, it was not required for viability or fertility of the flies, as the mutants were homozygous viable. Although Rh1 required Cnx for its expression, Cnx expression was normal in Rh1 mutants (Figure 2C, lane 7).

Mutations in *calnexin* Lead to Defects in Rhodopsin Maturation

Although Rh1 protein levels were severely reduced in the *cnx* mutants (Figure 2A, lanes 2 and 3), Rh1 transcript levels were normal in both (see Figure S1 in the Supplemental Data available online). These data suggest that Cnx functions post-transcriptionally and are consistent with a role for Cnx as a chaperone in Rh1 biosynthesis.

To investigate the role of Cnx in Rh1 biosynthesis, we assessed the kinetics of Rh1 maturation in the *cnx*^{1} mutant (Figure 3A). We utilized transgenic flies carrying the Rh1

gene under the control of a heat-shock promoter (hs) and tagged with an epitope corresponding to 12 amino acids at the C terminus of bovine rhodopsin (*hs-Rh1-bov transgene*) (Colley et al., 1995). The transgene was introduced into wt, cnx^1, and $ninaA^{P269}$ mutant flies. To initiate Rh1 biosynthesis, the transgenic flies were given a 1 hr heat-pulse at 37°C, shifted back to 22°C, and assayed at specific time points. We followed the fate of the heat-induced Rh1 protein by using a monoclonal antibody (1D4) directed to the epitope tag (bov). No Rh1 expression was detected in the flies prior to heat-pulse (Figure 3A, lane 1, no pulse). In wt flies, Rh1 was initially detected as immature high-MW forms that were converted to the mature low-MW form by 18 hr. In the cnx^1 mutant, Rh1 was also initially detected as immature high-MW forms but was significantly reduced by 24 hr. By 48 hr, very little Rh1 was detected, suggesting that most of the Rh1 was degraded.

The failure of Rh1 to mature in the cnx^1 mutant was similar to the fate of Rh1 in the *ninaA* mutant (Figure 3A). We have previously shown that NinaA is a chaperone specifically required for Rh1 biosynthesis and maturation (Baker et al., 1994; Colley et al., 1991). As in the cnx^1 mutant, Rh1 was initially detected as immature high-MW forms in the *ninaA* mutant. In contrast to the cnx^1 mutant, where most of the Rh1 was degraded, Rh1 accumulated in the immature high-MW form in the *ninaA* mutant.

We also followed the subcellular localization of Rh1 in the pulse-chase experiments (Figure 3B). In wt flies, by 8 hr following the heat-pulse, Rh1 immunolocalized to the ER in a perinuclear fashion, was detected in a punctate pattern consistent with transport vesicles, and was detected in the rhabdomeres. By 12 hr, more Rh1 was detected in the rhabdomeres, and by 24 hr, mature Rh1 localized solely to the rhabdomeres. This represents the normal progression for Rh1 maturation and transport through the secretory pathway. In the cnx^1 mutant, by 8 hr, Rh1 was detected predominantly in the ER. By 12 hr, Rh1 was still most noticeable in the ER. By 24 hr, Rh1 labeling was detected in both the ER and rhabdomeres, but was significantly fainter than wt. These results show that in the *cnx* mutant, while most Rh1 was degraded, some Rh1 successfully evaded the quality-control mechanisms and was transported to the rhabdomeres. In the *ninaA* mutants, at 8, 12, and 24 hr, Rh1 was detected primarily in the ER. A very small amount of Rh1 was detected in the rhabdomeres of *ninaA* mutants, again indicating that a small amount of Rh1 evaded the ER's quality-control system.

It is possible that Cnx and NinaA are part of a protein-processing pathway, ensuring proper folding and quality control of Rh1 during biosynthesis. To gain insights into the epistatic relationship between the two chaperones, we created mutant flies that were defective in both *cnx* and *ninaA*. The $ninaA^{P269};cnx^1$ double mutant displayed severely reduced levels of Rh1, comparable to those seen in the cnx^1 mutant alone (Figure 3C, lanes 4 and 2, respectively). These data demonstrate that in the double mutant, Rh1 was effectively degraded (as in *cnx*, Figure 3C, lane 2) rather than accumulating in the ER (as in *ninaA*, Figure 3C, lane 3). Therefore, *cnx* is epistatic to *ninaA*, as the phenotype of the *cnx* mutation overrides the phenotype of the *ninaA* mutation in the double mutant.

Because the two chaperones are required for Rh1 biosynthesis, we investigated the levels of NinaA protein in the *cnx* mutants. Figure 3D shows that the NinaA levels in *cnx* were indistinguishable from wt levels, suggesting that the defects in Rh1 were the result of a lack of Cnx, rather than a lack of NinaA.

Calnexin Associates with Rh1

The association of Cnx with Rh1 was assessed by coimmunoaffinity experiments (Baker et al., 1994). Cnx was isolated in a stable complex with Rh1 (Figure 3E, lane 2), but did not bind to or elute from the immunoaffinity column in the absence of Rh1 (extracts from the

Rh1 null allele, *ninaE*^{I17}) (Figure 3E, lane 3). These data indicated that Cnx and Rh1 physically associate in a protein complex, consistent with a role for Cnx as a molecular chaperone for Rh1.

Mutations in *calnexin* Lead to Retinal Degeneration

Examination of the *cnx* mutants revealed that they displayed an age-related retinal degeneration (Figure 4). Photoreceptor cells in 1-day-old *cnx* mutants displayed diminished rhabdomere size (Figure 4B) as compared to wt (Figure 4A). They also displayed accumulations of rough ER membranes, dilated Golgi, and various types of deposits (Figures 4B and 4C). These secretory pathway defects were consistent with a failure in Rh1 maturation. The identity of the deposits is unknown, but they may consist of degraded material within the cells. At 1 month, *cnx* mutants displayed a dramatic loss of rhabdomeres in the R1–6 photoreceptor cells, while the R7 and R8 photoreceptor cell rhabdomeres remained (Figures 4D and 4E, respectively). The *Drosophila* compound eye is made up of approximately 750 individual eye units called ommatidia. Each ommatidium contains eight photoreceptor cells (Figure 3B). Only R1–6 photoreceptors express Rh1, whereas R7 and R8 cells express a variety of different opsins (Rh3–6) (Chou et al., 1996; Montell et al., 1987; Papatsenko et al., 1997). The finding that only R1–6 rhabdomeres degenerated, and not R7 and R8, suggested that the opsins located in R7 and R8 were expressed normally.

Calnexin Is Uniquely Required by Rh1 in Photoreceptor Cells

To confirm normal expression of the minor rhodopsins in R7 and R8 cells, we performed immunocytochemical analysis of Rh3, Rh4, and Rh5 opsins in the *cnx* mutants. We found all three opsins to be correctly localized to the rhabdomeres of the R7 and R8 cells (Figure 5), confirming that while Cnx was required by Rh1, it was not required by the R7 and R8 opsins.

We examined whether ER processing of other photoreceptor proteins was defective in the *cnx* mutant. Immunocytochemical analysis revealed that another membrane protein, chaoptin, was present at its normal location in the rhabdomeres of the R1–8 photoreceptor cells in both *cnx* mutants (Figure 5D) and wt (Figure 5H). In addition, we performed immunoblotting analysis to confirm that a number of key phototransduction proteins, including the G protein α subunit (Gqα), the TRP and TRPL channels, PLC-β (*norpA*), arrestin 1 (Arr1), and arrestin 2 (Arr2) were all expressed at levels indistinguishable from wt (Figure 5I). These results demonstrated that while Cnx was required for processing of Rh1, it was not required for expression of these other photoreceptor cell proteins.

Calnexin Is an ER Protein in *Drosophila* Photoreceptors

To determine the expression pattern for Cnx, we generated polyclonal antibodies that recognized a 97 kDa band in wt flies that was not present in the mutants (Figure 2C). Cnx localized to the ER of all eight photoreceptor cells, often to ER cisternae that were tightly associated with the nuclear envelope (Figure 6). The labeling pattern for Cnx was compared to the ER proteins, $InsP_3R$ (inositol-1,3,5-trisphosphate receptor) and NinaA (Figure 6). All three proteins were expressed in the ER, but were absent from the rhabdomeres. Although the rhabdomeres of the central R7 photoreceptor cells were labeled by the $InsP_3R$ antibody, we previously showed this labeling to be nonspecific (Raghu et al., 2000). While Cnx protein was uniquely required by Rh1 in the R1–6 cells, it was detected in the ER of all eight photoreceptor cells (Figure 6).

Retinal Degeneration Is Light Dependent

To assess whether the retinal degeneration observed in the *cnx* mutants was enhanced by light activation of the phototransduction cascade, we reared the *cnx* mutants for 1 month in constant darkness. These flies displayed a less severe retinal degeneration (Figure 4F) compared with *cnx* mutants grown for1 month on a 12:12 light-dark cycle (Figures 4D and 4E). Therefore, activation of phototransduction by light enhanced the retinal degeneration in the *cnx* mutants. This result is contrasted to other known mutants defective in Rh1 maturation, such as *ninaA*, in which the retinal degeneration was light independent (Figures 4G and 4H) (Colley et al., 1991, 1995; Kurada and O'Tousa, 1995; Webel et al., 2000). In addition, the *ninaA* mutants degenerated more slowly compared to the *cnx* mutants (Figures 4D, 4E, and 4G).

The finding that light enhanced the retinal degeneration in the *cnx* mutant led us to investigate whether Ca^{2+} influx through the light-sensitive channels contributed to the retinal degeneration. Null mutations in the gene encoding the eye-enriched PLC (*norpA*) eliminate the light-induced Ca^{2+} influx. We generated *norpA;cnx* double mutants and found that *norpA* slowed down the onset and progression of the retinal degeneration in the *cnx* mutants (Figures 4I and 4J). The finding that the retinal degeneration in the *cnx* mutants was light enhanced and slowed by *norpA*, in combination with previous findings that calnexin binds Ca^{2+} (Tjoelker et al., 1994), prompted us to determine whether Cnx played a role in modulating Ca^{2+} in photoreceptor cells.

Mutations in *calnexin* Lead to Defects in Ca^{2+} Buffering

Current models of phototransduction suggest that virtually all aspects of excitation and adaptation are mediated within the microvilli. Because Cnx is located in the ER, we predicted that mutations in *cnx* would not affect the basic light responses, but might cause defects in Ca^{2+} buffering in the cell body. We first investigated the basic properties of the light-induced current (LIC) by using whole-cell patch-clamp recordings of photoreceptors from dissociated ommatidia to record the elementary responses (quantum bumps) representing the response to single-photon absorptions (Figure S2). In addition to wt flies, *ninaA* mutants were used as controls, because they express low (<1%) levels of functional Rh1 comparable to *cnx*, but unlike Cnx, the NinaA protein has no predicted Ca^{2+}-binding domains (Shieh et al., 1989). The most obvious phenotype in both *cnx* and *ninaA* was the great reduction in quantum capture (~100- to 200-fold), confirming the reduction in functional rhodopsin (Figure S2A and S2C). The quantum bump amplitude and waveform in *ninaA* and *cnx* were indistinguishable from each other, but both showed a significant (~50%) increase in quantum bump amplitude compared to wt (Figure S2A and S2B). A similar increase in quantum bump amplitudes has previously been described in Rh1 hypomorphs (Johnson and Pak, 1986). Otherwise, the quantum bump waveform in both *cnx* and *ninaA* was indistinguishable from wt. Macroscopic responses to brief test flashes and modest light steps in *cnx* and *ninaA* were also indistinguishable from each other, but greatly reduced in sensitivity compared to wt (data not shown). These results suggested that Cnx did not play a significant role in the basic light response and that, apart from the reduction in Rh1, all other key components of the phototransduction cascade were functional in both *cnx* and *ninaA*.

In order to measure Ca^{2+} levels in the cell body during illumination, we used the low-affinity Ca^{2+} indicator dye Fluo-4FF, loaded via the patch pipette. Wild-type, *ninaA*, and *cnx* photoreceptor cells were illuminated with the same intensity of 485 nm light, equivalent to ~10^8 effectively absorbed photons/s in wt flies (though only ~10^6 photons/s in *ninaA* and *cnx* because of the ~100-fold reduction in quantum catch). Even in *cnx* and *ninaA*, this corresponds to ~40 effectively absorbed photons/s per microvillus and appeared to be nearly

saturating, as a 7.5-fold brighter stimulus only induced slightly larger Ca^{2+} signals (Figure 7B). Fluorescence was measured from the entire cell, where the dominant contribution appears to come from the cell body. After an ~10– 20 ms latent period, which allows an estimate of F_{min} (see Experimental Procedures), the fluorescence increased to a peak after 200–300 ms and then declined to a steady-state plateau (Figure 7A). The absolute initial levels reached during this brief latent period in *cnx* and both wt and *ninaA* controls were indistinguishable, indicating that there was no systematic difference in dye loading or resting Ca^{2+} concentrations. However, both the maximum level reached and the plateau in *cnx* were approximately 2- to 3-fold higher than in either wt or *ninaA* controls (Figure 7A). The comparison with wt is particularly striking, because the effective intensity of illumination was 100-fold times greater in wt flies. We ruled out a reduction in the sacro-endoplasmic reticulum Ca^{2+} ATPase (SERCA) (Sanyal et al., 2005) or the Na^{+}/Ca^{2+} exchanger (CalX) (Wang et al., 2005) as being responsible for the increased Ca^{2+} as both proteins were expressed at wt levels in the *cnx* mutants (Figures 7C and 7D). The striking differences in the cytosolic Ca^{2+} signals between *cnx* and wt (and *ninaA*) indicated that Cnx played an important role in buffering Ca^{2+} in the cell body.

Discussion

Here, we demonstrate that Cnx plays a multifunctional role, serving as a chaperone for Rh1 and a regulator of Ca^{2+} during phototransduction. Furthermore, we provide genetic evidence that failure in Rh1 maturation and Ca^{2+} overload, resulting from defects in *cnx*, are responsible for retinal degeneration.

Rhodopsin Maturation and Retinal Degeneration

Calnexin serves a key role in glycoprotein folding and quality control in the ER and is thought to interact with a wide variety of newly synthesized proteins. Consistent with calnexin's broad substrate specificity, we show that it is ubiquitously expressed at all stages during development and in the adult. However, *cnx* mutants are homozygous viable and fertile, indicating that all proteins required for survival and reproduction fold sufficiently in the absence of Cnx. Cnx is, however, essential in the eye. We demonstrate that loss-of-function mutations in *cnx* lead to defects in Rh1 maturation and cause age-dependent retinal degeneration. Although Cnx is essential for Rh1 biosynthesis, it is not required for the expression or function of other photoreceptor cell proteins. This indicates that even within the eye, Cnx may play a unique role. There are two possible explanations for the specific requirement for Cnx by Rh1. First, chaperones with redundant functions may compensate for the loss of Cnx. Second, Cnx may serve as a chaperone that is exclusively dedicated to Rh1.

With the exception of Rh1, photoreceptor cell proteins manage to fold normally in cells lacking calnexin. This could be due to redundancy between folding factors in the ER. For example, calreticulin (located on 3R, 85E) as well as two additional *calnexin* genes (*cnx11* and *cnx14*) are present in *Drosophila* (Hong and Ganetzky, 1996). These chaperones may compensate for the lack of calnexin function in all cases except during Rh1 biosynthesis. An alternative conclusion is that Cnx may be exclusively devoted to Rh1. Consistent with this scenario, another chaperone, NinaA, is also expressed in all eight photoreceptor cells yet is specifically dedicated to Rh1 biosynthesis in the R1–6 photoreceptor cells (Colley et al., 1991; Stamnes et al., 1991). In addition, a cyclophilin-like protein expressed in the mammalian retina, RanBP2, acts as a specific chaperone for red/green opsin (Ferreira et al., 1996). Given the importance and abundance of rhodopsin, it is plausible that Cnx and NinaA are part of a system of chaperones that is dedicated to its folding and quality control.

Consistent with results presented here, calnexindeficient mice have been generated that are homozygous viable. Half die within the first 2 days, and those that survive are smaller than their littermates, develop severe motor disorders, and display a dramatic loss of large myelinated nerve fibers (Denzel et al., 2002). Mice contain a single calnexin gene, eliminating the possibility of redundancy between calnexins. However, it is possible that calreticulin is able to partially compensate for the loss of calnexin in utero and in adults, but is unable to compensate for all calnexin functions.

Calnexin Functions in Ca^{2+} Regulation in the Cytosol

We found that photoreceptor cells in the *cnx* mutants display elevated and sustained cytosolic Ca^{2+} levels following light stimulation, consistent with a role for Cnx in buffering Ca^{2+}. Calnexin's cytosolic domain displays structural similarity to calreticulin's highly charged C domain, but is positioned on the opposite side of the ER membrane (Tjoelker et al., 1994). Calreticulin's C domain displays low-affinity, high-capacity Ca^{2+}-binding properties and plays a major role in Ca^{2+} modulation in the lumen of the ER (Baksh and Michalak, 1991). Given their structural similarity, we propose that calnexin's C domain serves a similar function in modulating Ca^{2+}, but in the cyotosol. These low-affinity and high-capacity Ca^{2+}-binding properties would make calnexin's cytosolic domain ideal for buffering high levels of Ca^{2+} in the photoreceptors. We propose that Cnx serves to buffer Ca^{2+} that diffuses into the cell body after entering via the light-sensitive TRP and TRPL channels.

The *Drosophila* compound eye has emerged as an important model for unraveling the mechanisms of retinal degeneration and phototransduction. Retinal degeneration can be triggered by mutations in almost every protein that functions in phototransduction. Although the mechanisms for each are not well understood, these mutations can be divided into at least two distinct classes. One involves protein maturation defects, most commonly in rhodopsin (Colley et al., 1995; Kurada and O'Tousa, 1995), and the other involves a combination of unregulated activities of the phototransduction cascade and/or Ca^{2+} toxicity (Wang et al., 2005). Retinal degeneration caused by defects in rhodopsin folding does not require light activation of phototransduction and is therefore light independent. However, retinal degenerations stemming from unregulated phototransduction or Ca^{2+} toxicity are dependent on light stimulation of the cascade and opening of the light-sensitive TRP and TRPL channels. Genetic analysis has revealed a number of mutants that fall into one class or the other, but very few that exhibit both properties (Georgiev et al., 2005). The *cnx* mutants clearly display defects in Rh1 maturation, and yet they also undergo a light-enhanced retinal degeneration. This indicates that defects in Rh1 maturation are not solely responsible for the retinal degeneration. Our results, indicating impaired Ca^{2+} buffering in the *cnx* mutants, along with the ability of the *norpA* mutation to partially prevent degeneration in *cnx*, suggests that Ca^{2+} toxicity also contributes to the retinal degeneration. Therefore, we propose that the *cnx* mutant displays characteristics of two distinct classes of retinal degeneration; one involving defects in Rh1 maturation, and the other involving Ca^{2+} toxicity.

These results provide genetic evidence that failure in Rh1 maturation and Ca^{2+} overload, resulting from defects in Cnx, are responsible for retinal degeneration. Because calnexin has been localized to the ER of photoreceptor cells in mice, it may play a protein-folding role in the mammalian retina as well as in *Drosophila* (Frederick et al., 2001). Furthermore, because *Drosophila cnx* displays 49% amino acid identity with human *calnexin* (Figure 1B), mutations identified in *Drosophila calnexin* may be clinically relevant to hereditary human retinal degeneration diseases.

Experimental Procedures

Genetic Screen, *Drosophila* Strains, and Transgenic Animals

We screened ~12,000 ethyl methyl sulfonate (EMS)-mutagenized lines obtained from the Zuker collection (Koundakjian et al., 2004). The genotype of the parental wild-type stock used for the mutagenesis was *w+; brown (bw); scarlet (st)*. Using this approach, homozygotes were easily selected from heterozygotes based on their white eye color. To identify potential candidate genes relevant to retinal degeneration, we screened homozygous adult eyes for the presence or absence of the deep pseudopupil (DPP), which is a reliable indicator of the structural integrity of the photoreceptor cells (Franceschini, 1972; Franceschini and Kirschfeld, 1971). We identified ~900 DPP-defective lines from which two independent *calnexin* alleles were obtained (cnx^1 and cnx^2). The red-eyed wt strain used in these studies was *Drosophila melanogaster* Canton-S and the white-eyed wt strains used were w^{1118} and the parental line, *w+; bw; st*. Other fly stocks include $ninaA^{P269}$, $ninaE^{I17}$, $norpA^{P24}$, and eya^1. *Drosophila* stocks with deficiencies uncovering 99A and the duplication were obtained from the Bloomington Stock Center. The $ninaA^{P269}; cnx^1$ double mutants and $norpA^{P24}; cnx^1$ double mutants were created by using standard *Drosophila* techniques. We used transgenic flies expressing wild-type Rh1 tagged with a 12 amino acid epitope tag at the C terminus *P[Rh1-bov]* (Colley et al., 1995). This epitope tag does not affect Rh1 maturation or function (Colley et al., 1995). For heat pulse-chase experiments, we used transgenic flies expressing the Rh1-bov construct under the control of the *Drosophila Hsp70 heat-shock promoter, P[hs-Rh1-bov]* (Colley et al., 1995).

Sequencing and Alignment

Genomic DNA was isolated from the two mutant *Drosophila* lines (cnx^1 and cnx^2) and the parental wt line (*bw; st*) by using standard DNA isolation techniques (Dolph et al., 1993). Primers spanning the *cnx* gene were designed based on the GenBank sequence accession number CG11958 (Brody et al., 2002; Christodoulou et al., 1997). DNA sequence was determined by fluorescent-based sequencing methods, and sequence was analyzed and aligned as previously described (Haug-Collet et al., 1999).

Northern Blot Analysis

Total RNA was prepared from the heads and bodies of 0- to 7-day-old *Drosophila* Canton-S, *bw; st*, cnx^1, cnx^2, and eya^1 lines by using the Ultraspec RNA isolation system (Biotecx, Houston, TX). Poly(A)$^+$ RNA was obtained by using the Poly(A)Pure mRNA purification kit (Ambion, Austin, TX). Poly(A)$^+$ RNA from third instar larvae and 0– 24 hr embryos (Canton-S strain) was purchased from Clontech (Palo Alto, CA). Poly(A)$^+$ RNA (10 μg) was run on denaturing 1% agarose gels that were processed and transferred to a positively charged nylon membrane as previously described (Haug-Collet et al., 1999). The DIG-labeled probe consisted of a 2.1 Kb XhoI/EcoRI fragment, containing the entire *cnx* cds (EST GH03249) (Rubin et al., 2000). A DIG-labeled actin RNA probe was used as an internal control for loading (Roche, Indianapolis, IN). Northern blots were carried out in young *cnx* mutant flies, prior to retinal degeneration.

SDS-PAGE, Immunoblotting, and Affinity Chromatography

Fly head samples were separated by electrophoresis in 12% SDS-polyacrylamide gels and electroblotted onto nitrocellulose membranes as previously described (Colley et al., 1991). In all experiments, nitrocellulose membranes were stained with 0.05% Ponceau S to ensure that each lane contained the appropriate amount of protein. The 4C5 monoclonal antibody directed to Rh1 and the tubulin antibody were obtained from the Developmental Studies Hybridoma Bank, Iowa. Rh1 containing the bov-epitope tag was detected by using the 1D4

mouse monoclonal antibody (MacKenzie et al., 1984; Oprian et al., 1987). The following rabbit polyclonal antibodies were a gift from A. Becker and C.S. Zuker: NinaA (Baker et al., 1994; Colley et al., 1991; Stamnes et al., 1991), G-α subunit of DGq (Scott et al., 1995), Trp and Trpl light-sensitive channels (Niemeyer et al., 1996), NorpA (phospholipase C-β) (Tsunoda et al., 1997), arrestin1 (Arr1) and arrestin2 (Arr2) (Dolph et al., 1993). The antibody directed to SERCA was a gift from M. Ramaswami (Sanyal et al., 2005), and CalX was a gift from C. Montell (Wang et al., 2005). The immunoreactive proteins were visualized by using horseradish peroxidase-conjugated goat anti-mouse or anti-rabbit IgG (Jackson ImmunoResearch, Westgrove, PA) followed by ECL detection (Amersham Pharmecia Biotech, Piscataway, NJ). Immunoblotting was carried out in young flies, prior to retinal degeneration.

Flies were subjected to affinity chromatography essentially as we have previously described (Baker et al., 1994) by using ~3000 heads for wild-type(w^{1118}) and $ninaE^{I17}$ flies. Membranes were prepared by centrifugation at 100,000 × g for 60 min. The membrane pellet was suspended in sodium phosphate buffer containing 1% n-dodecylβ-D-maltoside, homogenized and centrifuged at 150,000 × g for 60 min to remove insoluble material. The supernatant was loaded onto columns of CNBr activated Sepharose 4B (Amersham-Pharmacia, Inc.) conjugated to 4C5 mouse monoclonal antibody directed to Rh1. After exhaustive rinsing, Rh1 and its associated proteins were eluted with triethylamine (pH 11.2). The samples were dialyzed, concentrated, and suspended in sample buffer (Laemmli, 1970) before being subjected to SDS-PAGE and immunoblotting. The eluted sample was divided such that 88% of the sample was used for detection of Cnx using the rabbit polyclonal antibody and 12% of sample was used for detection of Rh1 using the 4C5 mouse monoclonal antibody.

Generation of Anti-Calnexin Antibodies

A polyclonal rabbit antibody directed to Cnx was created that corresponded to a 24 amino acid peptide at the C terminus of the Cnx protein. The peptide consisted of NH_2-ESREPAQTEESNTKTRKRQAR KEK-COOH corresponding to amino acid numbers 583–605. The peptide carried a terminal lysine residue to facilitate glutaraldehyde conjugation to the immunogenic reagent, keyhole limpet hemocyanin (KLH) (Pierce Biotechnology, Inc. Rockford, IL). The antibodies were generated in rabbits by Cocalico Biologicals (Reamstown, PA).

Immunocytochemistry

Immunocytochemistry was carried out according to Colley et al. (Colley et al., 1991). Frozen 0.5 μm sections were immunolabeled with the 4C5 and 1D4 monoclonal antibodies directed to Rh1 and the bov-epitope tag, respectively (de Couet and Tanimura, 1987; MacKenzie et al., 1984; Oprian et al., 1987). A polyclonal antibody directed to Cnx was generated (see above). Monoclonal mouse antibodies directed to Rh3, Rh4, and Rh5 were provided by S. Britt (Chou et al., 1996). The antibody directed to chaoptin (24B10) was obtained from D. Van Vactor and S.L. Zipursky (Reinke et al., 1988). The polyconal antibodies directed to the NinaA protein were provided by A. Becker and C.S. Zuker (Colley et al., 1991). The $InsP_3R$ antibody was provided by M. Danin and Z. Selinger (Padinjat et al., 2000). Primary antibody labeling was detected by fluorescein-conjugated goat anti-mouse or Texas red-conjugated goat anti-rabbit (Jackson ImmunoResearch). Nuclei were labeled with ToPro-3 nucleic acid stain (Molecular Probes, Inc., Eugene, OR). Sections were viewed using a BioRad MRC1024 laser scanning confocal microscope (BioRad Laboratories, Life Sciences Division, Hercules, CA). For each experiment, at least five individual heads were sectioned and between 50 to 100 ommatidia were observed in each eye. Immunocytochemistry was carried out in young flies, prior to retinal degeneration.

Electron Microscopy

For electron microscopy, adult heads were fixed and processed according to a modification of the methods of Baumann and Walz (Baumann et al., 1994) as previously described (Colley et al., 1991, 1995). Ultrathin sections were stained with 2% uranyl acetate and lead citrate, and viewed at 80 kV on a Phillips CM120 electron microscope. For all genotypes described, at least three individual heads were sectioned and 50 to 100 ommatidia were observed in each eye. During initial phases of the study, serial sections were obtained from mutant flies to ensure that the phenotype was consistent from the apical to the basal regions of the eye.

Whole-Cell Recordings and Ca^{2+} Measurements

Dissociated ommatidia were prepared as previously described (Hardie, 1991, 2001) from recently eclosed adult flies and transferred to a recording chamber on an inverted Nikon Diaphot microscope. The bath was composed of 120 mM NaCl, 5 mM KCl, 10 mM TES, 4 mM $MgCl_2$, 1.5 mM $CaCl_2$, 25 mM proline, and 5 mM alanine. The intracellular pipette solution was 140 mM K gluconate, 10 mM TES, 4 mM Mg ATP, 2 mM $MgCl_2$, 1 mM NAD, and 0.4 mM Na^+-GTP. The pH of both solutions was 7.15 (Figure S2). Measurements of cytosolic Ca^{2+} were performed using the single-wavelength low-affinity Ca^{2+} indicator dye fluo-4FF (nominal Kd 9.7 μM, Molecular Probes) loaded via the pipette at 100 micromolar. Cells were illuminated for 2 s with 485 nm excitation delivered via a Uniblitz shutter (rise time < 2 ms) from a 75 W Xe arc lamp corresponding to an intensity of ~1×10^8 effective rhodopsin isomerizations/s in wt flies. Background-subtracted fluorescence values were expressed as ΔF/ F min, where ΔF is the increase in fluorescence above the basal (Fmin) fluorescence level. The low affinity of Fluo-4FF means that the resting cytosolic concentration of ~150 nM (Hardie, 1996b) should be close to Fmin levels for this dye. Because it was impractical to lower Ca^{2+} further than this, in all cells Fmin was arbitrarily assumed to be 80% of the minimum value measured during the finite latent period (~10–20 ms) at light onset when Ca^{2+} levels are still at the dark resting level (Hardie, 1996b). The maximal fluorescence signal (Fmax) was estimated in a few cells (n = 4) recorded with 20 mM internal Na^+ in the electrode, by subsequently perfusing cells with a solution containing 90 mM LiCl and 20 mM NaCl and 1.5 mM Ca^{2+} (to drive reverse Na^+/ Ca^{2+} exchange) in addition to the Ca^{2+} ionophore ionomycin (14 μM). The maximum values reached were approximately three to four times greater (3.68 6 0.74) than the maximal light-induced values (in *cnx* flies), indicating that all measurements were well within the dynamic, quasilinear range of the dye.

Supplementary Material

Refer to Web version on PubMed Central for supplementary material.

Acknowledgments

We thank Drs. M.A. Basso, C. Desplan, L. Levin, M. Michalak, and A. Polans, as well as Ms. N. Rozas, for valuable discussions and comments on the manuscript. The authors thank T. Abell, K. Benton, J. Newman, C. Rockwell, J. Rocky, and R. Ward for their expert technical assistance, as well as B. Krieber, B. Hardy, and Dr. B. Ganetzky for assistance with fly stocks. Dr. S. Britt generously provided DNA for the transformations and the antibodies directed to Rh3, Rh4, Rh5. Dr. K. Moses assisted with the production of the transgenic flies. Drs. M. Ramaswami and C. Montell provided antibodies directed to SERCA and CalX, respectively. Dr. P. Robinson provided the 1D4 antibody and Dr. C.S. Zuker and A. Leslie generously provided several antibodies directed to the *Drosophila* photoreceptor proteins. Drs. D. VanVactor and L. Zipursky provided the antibody directed to chaoptin. We are grateful to J. Harder for his assistance with the computer graphics. Dr. C.S. Zuker generously provided us with the opportunity to screen the EMS-generated alleles from the Zuker Collection. Drs. S. Carroll and S. Paddock generously provided their expertise and use of the confocal microscope. This work was supported by NIH EY08768, Retina Research Foundation, HHMI, and the RPB foundation to N.J.C.

References

Baker EK, Colley NJ, Zuker CS. The cyclophilin homolog NinaA functions as a chaperone, forming a stable complex in vivo with its protein target rhodopsin. EMBO J. 1994; 13:4886–4895. [PubMed: 7957056]

Baksh S, Michalak M. Expression of calreticulin in Escherichia coli and identification of its Ca2+ binding domains. J. Biol. Chem. 1991; 266:21458–21465. [PubMed: 1939178]

Baumann O, Lautenschlager B, Takeyasu K. Immuno-localization of Na,K-ATPase in blowfly photoreceptor cells. Cell Tissue Res. 1994; 275:225–234. [PubMed: 8111836]

Brody T, Stivers C, Nagle J, Odenwald WF. Identification of novel Drosophila neural precursor genes using a differential embryonic head cDNA screen. Mech. Dev. 2002; 113:41–59. [PubMed: 11900973]

Chou WH, Hall KJ, Wilson DB, Wideman CL, Townson SM, Chadwell LV, Britt SG. Identification of a novel *Drosophila* opsin reveals specific patterning of the R7 and R8 photoreceptor cells. Neuron. 1996; 17:1101–1115. [PubMed: 8982159]

Christodoulou S, Lockyer AE, Foster JM, Hoheisel JD, Roberts DB. Nucleotide sequence of a *Drosophila* melanogaster cDNA encoding a calnexin homologue. Gene. 1997; 191:143–148. [PubMed: 9218712]

Colley NJ, Baker EK, Stamnes MA, Zuker CS. The cyclophilin homolog ninaA is required in the secretory pathway. Cell. 1991; 67:255–263. [PubMed: 1913822]

Colley NJ, Cassill JA, Baker EK, Zuker CS. Defective intracellular transport is the molecular basis of rhodopsin-dependent dominant retinal degeneration. Proc. Natl. Acad. Sci. USA. 1995; 92:3070–3074. [PubMed: 7708777]

de Couet HG, Tanimura T. Monoclonal antibodies provide evidence that rhodopsin in the outer rhabdomeres of *Drosophila melanogaster* is not glycosylated. Eur. J. Cell Biol. 1987; 44:50–56.

Denzel A, Molinari M, Trigueros C, Martin JE, Velmurgan S, Brown S, Stamp G, Owen MJ. Early postnatal death and motor disorders in mice congenitally deficient in calnexin expression. Mol. Cell. Biol. 2002; 22:7398–7404. [PubMed: 12370287]

Dolph PJ, Ranganathan R, Colley NJ, Hardy RW, Socolich M, Zuker CS. Arrestin function in inactivation of G protein-coupled receptor rhodopsin in vivo. Science. 1993; 260:1910–1916. [PubMed: 8316831]

Ellgaard, L.; Helenius, A. Calreticulin. New York: Kluwer Academic/Plenum Publishers; 2003a. A Chaperone System For Glycoprotein Folding: The Calnexin/Calreticulin Cycle; p. 19-30.

Ellgaard L, Helenius A. Quality control in the endoplasmic reticulum. Nat. Rev. Mol. Cell Biol. 2003b; 4:181–191. [PubMed: 12612637]

Fain GL, Lisman JE. Light, Ca2+, and photoreceptor death: New evidence for the equivalent-light hypothesis from arrestin knockout mice. Invest. Ophthalmol. Vis. Sci. 1999; 40:2770–2772. [PubMed: 10549634]

Ferreira PA, Nakayama TA, Pak WL, Travis GH. Cyclophilin-related protein RanBP2 acts as chaperone for red/green opsin. Nature. 1996; 383:637–640. [PubMed: 8857542]

Franceschini, N. Pupil and pseudopupil in the compound eye of Drosophila. In: Wehner, R., editor. Information Processing in the Visul Systems of Arthropods. Berlin: Springer-Verlag; 1972. p. 75-82.

Franceschini N, Kirschfeld K. Pseudopupil phenomena in the Drosophila compound eye. Kybernetik. 1971; 9:159–182. [PubMed: 5134358]

Frederick JM, Krasnoperova NV, Hoffmann K, Church-Kopish J, Ruther K, Howes K, Lem J, Baehr W. Mutant Rhodopsin Transgene Expression on a Null Background. Invest. Ophthalmol. Vis. Sci. 2001; 42:826–833. [PubMed: 11222546]

Georgiev P, Garcia-Murillas I, Ulahannan D, Hardie RC, Raghu P. Functional INAD complexes are required to mediate degeneration in photoreceptors of the Drosophila rdgA mutant. J. Cell Sci. 2005; 118:1373–1384. [PubMed: 15755798]

Hardie RC. Whole-cell recordings of the light induced current in dissociated *Drosophila* photoreceptors: evidence for feedback by calcium permeating the light-sensitive channels. Proc. R Acad. Sci. Lond. B Biol. Sci. 1991; 245:203–210.

Hardie RC. Excitation of *Drosophila* photoreceptors by BAPTA and ionomycin: evidence for capacitative Ca2+ entry? Cell Calcium. 1996a; 20:315–327. [PubMed: 8939351]

Hardie RC. INDO-1 measurements of absolute resting and light-induced Ca^{2+} concentration in *Drosophila* photoreceptors. J. Neurosci. 1996b; 16:2924–2933. [PubMed: 8622123]

Hardie RC. Phototransduction in Drosophila melanogaster. J. Exp. Biol. 2001; 204:3403–3409. [PubMed: 11707492]

Hardie RC, Raghu P. Visual transduction in Drosophila. Nature. 2001; 413:186–193. [PubMed: 11557987]

Haug-Collet K, Pearson B, Webel R, Szerencsei RT, Winkfein RJ, Schnetkamp PPM, Colley NJ. Cloning and characterization of a potassium-dependent sodium/calcium exchanger in *Drosophila*. J. Cell Biol. 1999; 147:659–669. [PubMed: 10545508]

Hong CS, Ganetzky B. Molecular characterization of neurally expressing genes in the para sodium channel gene cluster of Drosophila. Genetics. 1996; 142:879–892. [PubMed: 8849894]

Johnson EC, Pak WL. Electrophysiological study of *Drosophila* rhodopsin mutants. J. Gen. Physiol. 1986; 88:651–673. [PubMed: 3097245]

Koundakjian EJ, Cowan DM, Hardy RW, Becker AH. The Zuker collection: A resource for the analysis of autosomal gene function in Drosophila melanogaster. Genetics. 2004; 167:203–206. [PubMed: 15166147]

Kurada P, O'Tousa JE. Retinal degeneration caused by dominant rhodopsin mutations in *Drosophila*. Neuron. 1995; 14:571–579. [PubMed: 7695903]

Kyte J, Doolittle RF. A simple model for displaying the hydropathic character of a protein. J. Mol. Biol. 1982; 157:105–132. [PubMed: 7108955]

Laemmli UK. Cleavage of structural proteins during assembly of the head of bacteriophage T4. Nature. 1970; 227:680–685. [PubMed: 5432063]

MacKenzie D, Arendt A, Hargrave P, McDowell JH, Molday RS. Localization of binding sites for carboxyl terminal specific anti-rhodopsin monoclonal antibodies using synthetic peptides. Biochemistry. 1984; 23:6544–6549. [PubMed: 6529569]

Molinari M, Eriksson KK, Calanca V, Galli C, Cresswell P, Michalak M, Helenius A. Contrasting functions of calreticulin and calnexin in glycoprotein folding and ER quality control. Mol. Cell. 2004; 13:125–135. [PubMed: 14731400]

Montell C, Jones K, Zuker C, Rubin G. A second opsin gene expressed in the ultraviolet-sensitive R7 photoreceptor cells of *Drosophila* melanogaster. J. Neurosci. 1987; 7:1558–1566. [PubMed: 2952772]

Muchowski PJ, Wacker JL. Modulation of Neurodegeneration by molecular chaperones. Nat. Rev. Neurosci. 2005; 6:11–22. [PubMed: 15611723]

Niemeyer BA, Suzuki E, Scott K, Jalink K, Zuker CS. The *Drosophila* light-activated conductance is composed of the two channels TRP and TRPL. Cell. 1996; 85:651–659. [PubMed: 8646774]

Oberwinkler J, Stavenga DG. Calcium imaging demonstrates colocalization of calcium influx and extrusion in fly photoreceptors. Proc. Natl. Acad. Sci. USA. 2000; 97:8578–8583. [PubMed: 10900015]

Oprian DD, Molday RS, Kaufman RJ, Khorana HG. Expression of a synthetic bovine rhodopsin gene in monkey kidney cells. Proc. Natl. Acad. Sci. USA. 1987; 84:8874–8878. [PubMed: 2962193]

Pacione LR, Szego MJ, Ikeda S, Nishina PM, McInnes RR. Progress toward understanding the genetic and biochemical mechansims of inherited photoreceptor degenerations. Annu. Rev. Neurosci. 2003; 26:657–700. [PubMed: 14527271]

Padinjat R, Colley NJ, Webel R, James T, Hasan G, Selinger Z, Hardie RC. Normal phototransduction in *Drosophila* photoreceptors lacking an InsP3 receptor gene. Mol. Cell. Neurosci. 2000; 15:429–445. [PubMed: 10833300]

Pak W, Leung H. Genetic approaches to visual transduction in Drosophila melanogaster. Receptors Channels. 2003; 9:149–167. [PubMed: 12775337]

Papatsenko D, Sheng G, Desplan C. A new rhodopsin in R8 photoreceptors of *Drosophila*: evidence for coordinate expression with Rh3 in R7 cells. Development. 1997; 124:1665–1673. [PubMed: 9165115]

Postma M, Oberwinkler J, Stavenga DG. Does Ca2+ reach millimolar concentrations after single photon absorption in Drosophila photoreceptor microvilli? Biophys. J. 1999; 77:1811–1823. [PubMed: 10512805]

Raghu P, Colley NJ, Webel R, James T, Hasan G, Danin M, Selinger Z, Hardie RC. Normal Phototransduction in Drosophila Photoreceptors Lacking an InsP3 Receptor. Gene. Mol. Cell. Neurosci. 2000; 15:429–445.

Reinke R, Krantz DE, Yen D, Zipursky SL. Chaoptin, a cell surface glycoprotein required for *Drosophila* photoreceptor cell morphogenesis, contains a repeat motif found in yeast and human. Cell. 1988; 52:291–301. [PubMed: 3124963]

Rubin GM, Hong L, Brokstein P, Evans-Holm M, Frise E, Stapleton M, Harvey DA. A *Drosophila* complementary DNA resource. Science. 2000; 287:2222–2224. [PubMed: 10731138]

Sanyal S, Consoulas C, Kuromi H, Basole A, Mukai L, Kidokoro Y, Krishnan KS, Ramaswami M. Analysis of conditional paralytic mutants in Drosophila sarco-endoplasmic reticulum calcium ATPase reveals novel mechanisms for regulating membrane excitability. Genetics. 2005; 169:737–750. [PubMed: 15520268]

Schrag JD, Bergeron JJM, Li Y, Borisova S, Hahn M, Thomas DY, Cygler M. The structure of calnexin, an ER chaperone involved in quality control of protein folding. Mol. Cell. 2001; 8:633–644. [PubMed: 11583625]

Scott K, Becker A, Sun Y, Hardy R, Zuker C. Gq alpha protein function in vivo: genetic dissection of its role in photoreceptor cell physiology. Neuron. 1995; 15:919–927. [PubMed: 7576640]

Shieh BH, Stamnes MA, Seavello S, Harris GL, Zuker CS. The *ninaA* gene required for visual transduction in *Drosophila* encodes a homologue of cyclosporin A-binding protein. Nature. 1989; 338:67–70. [PubMed: 2493138]

Stamnes MA, Shieh BH, Chuman L, Harris GL, Zuker CS. The cyclophilin homolog ninaA is a tissue-specific integral membrane protein required for the proper synthesis of a subset of *Drosophila* rhodopsins. Cell. 1991; 65:219–227. [PubMed: 1707759]

Sung CH, Tai AW. Rhodopsin trafficking and its role in retinal dystrophies. Int. Rev. Cytol. 2000; 195:215–267. [PubMed: 10603577]

Tjoelker LW, Seyfried CE, Eddy RL, Byers MG, Shows TB, Calderon J, Schreiber RB, Gray PW. Human, mouse, and rat calnexin cDNA cloning: identification of potential calcium binding motifs and gene localization to human chromosome 5. Biochemistry. 1994; 33:3229–3236. [PubMed: 8136357]

Tsunoda S, Sierralta J, Sun Y, Bodner R, Suzuki E, Becker A, Socolich M, Zuker CS. A multivalent PDZ-domain protein assembles signalling complexes in a G-protein-coupled cascade. Nature. 1997; 388:243–249. [PubMed: 9230432]

Wang T, Xu H, Oberwinkler J, Gu Y, Hardie RC, Montell C. Light activation, adaptation, and cell survival functions of the Na+/Ca2+ exchanger CalX. Neuron. 2005; 45:367–378. [PubMed: 15694324]

Ware FE, Vassilakos A, Peterson PA, Jackson MR, Lehrman MA, Williams DB. The molecular chaperone calnexin binds Glc1Man9GlcNAc2 oligosaccharide as an initial step in recognizing unfolded glycoproteins. J. Biol. Chem. 1995; 270:4697–4704. [PubMed: 7876241]

Webel R, Menon I, O'Tousa J, Colley NJ. Role of asparagine-linked glycosylation sites in rhodopsin maturation and association with its molecular chaperone, NinaA. J. Biol. Chem. 2000; 275:24752–24759. [PubMed: 10811808]

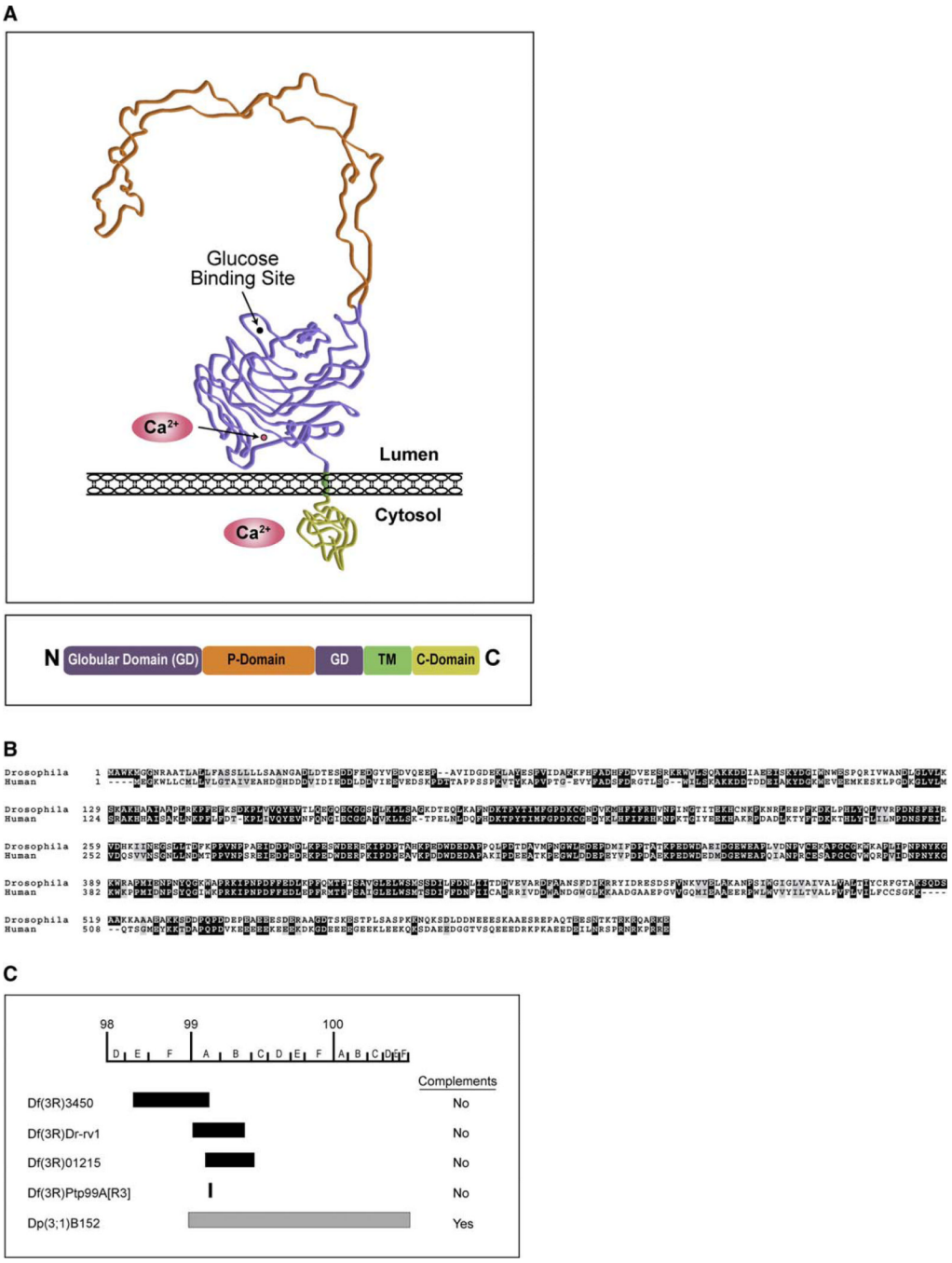

Figure 1. ***Drosophila*** **Calnexin**

(A) Proposed structure of Cnx. (Top box) A schematic of the proposed three-dimensional structure for Cnx based on crystallization of the luminal domain of canine calnexin (Schrag et al., 2001). (Bottom box) The proposed domain structure of the *Drosophila* Cnx protein, showing the N-terminal luminal domains (amino acid numbers 1–489), the transmembrane (TM) domain (amino acid numbers 490–508), and the cytosolic domain (amino acid numbers 509–605). It has been proposed that the luminal domain contains two distinct regions: a compact, globular domain (purple) and a proline-rich arm called the P domain (orange) (Schrag et al., 2001). Shown are the proposed Ca^{2+}-binding (Ca^{2+}) and glucose-binding sites within the globular domain. The TM segment (green) was identified based on

hydropathy plot analysis of the conceptual Cnx protein using the Kyte-Doolittle algorithm (Kyte and Doolittle, 1982) (data not shown). The carboxyl-terminal cytosolic domain (yellow) is highly charged and effectively binds Ca^{2+} (Tjoelker et al., 1994).
(B) *Drosophila cnx* encodes a 605 amino acid protein that displays 49% identity with human calnexin (chromosome 5q). Clustal/W amino acid alignment between *Drosophila* Cnx and human calnexin (CNX). Dark shading indicates identity, whereas light shading indicates similarity. Numbers refer to amino acids.
(C) *Drosophila* deficiencies and duplications corresponding to *cnx* are shown. The following deficiencies failed to complement the *cnx* alleles: Df(3R)3450 uncovers 98E3 to 99A6-8, Df(3R)Dr-rv1 uncovers 99A1-2 to 99B6-11, Df(3R)01215 uncovers 99A6 to 99C1, Df(3R)Ptp99A[R3] uncovers 99A7. A *Drosophila* stock with a duplication for 98F14 to 100F and translocation to the X chromosome [Dp(3;1)B152] positively complemented the *cnx* alleles.

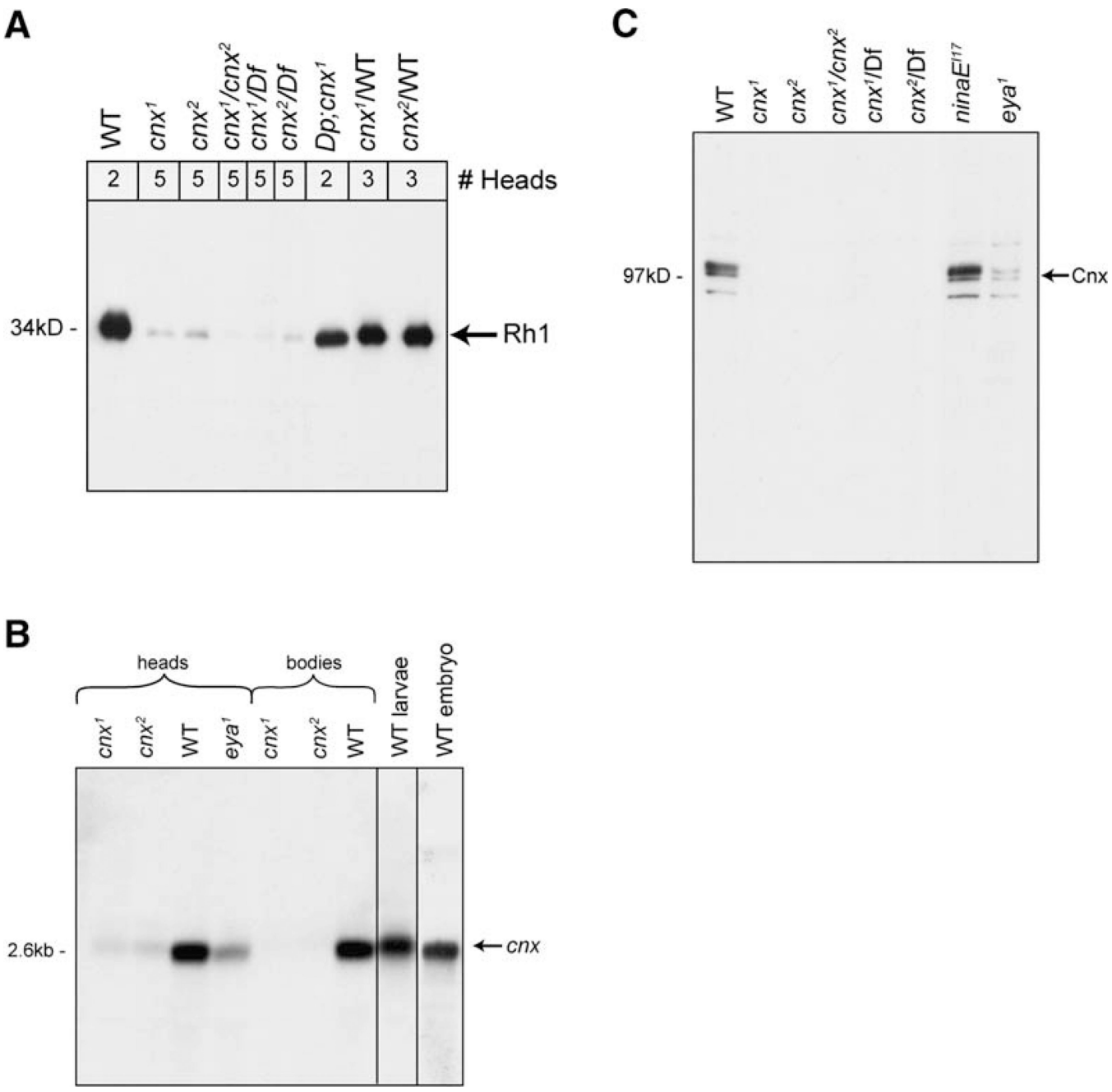

Figure 2. Characterization of *calnexin* Mutant in *Drosophila*

(A) Rh1 protein was severely reduced in both *cnx* mutants. Immunoblot of proteins isolated from heads of young flies prior to retinal degeneration (0–4 days old) were labeled with a monoclonal antibody directed to Rh1 (4C5). (1) Wild-type (*bw;st*), (2) cnx^1, (3) cnx^2, (4) cnx^1/cnx^2 transheterozygote, (5 and 6) cnx^1 and cnx^2 mutants in *trans* to a deficiency (Df) that eliminates 99A (Bloomington stock, Df(3R)Ptp99A[R3]), (7) cnx^1 complemented by the duplication for 99A (Bloomington stock, Dp(3;1) B152), and (8 and 9) cnx^1 and cnx^2 heterozygotes, respectively (carried over a wt chromosome). Nitrocellulose membranes were stained with Ponceau S to ensure that each lane contained the appropriate amount ofprotein. Numbers at the top refer to the number of fly heads loaded per lane. We loaded more heads in the mutant lanes because very little Rh1 protein was expressed.

(B) Cnx transcript was severely reduced in both *cnx* mutants. Northern blot analysis revealed that *cnx* encodes a 2.6 kb transcript. (1) cnx^1 heads, (2) cnx^2 heads, (3) wt heads, (4) heads from flies lacking eyes (eya^1), (5) cnx^1 bodies, (6) cnx^2 bodies, (7) wt bodies, (8) wt larvae, and (9) wt embryos. mRNA was isolated from 0- to 7-day-old *cnx* mutants, prior to retinal degeneration. Ten micrograms of $polyA^+$ selected RNA was loaded into each lane. An internal control for loading was a DIG-labeled actin RNA probe (not shown) (Roche, Indianapolis, IN). The wt strain used was Canton S.

(C) Cnx protein was absent in the *cnx* mutants. Immunoblot labeled with a polyclonal antibody directed to Cnx detected a 97 kDa band. (1) Wild-type (*bw;st*), (2) cnx^1, (3) cnx^2, (4) cnx^1/cnx^2 transheterozygote, (5 and 6) cnx^1 and cnx^2 mutants in *trans* to a deficiency (Df) that eliminates 99A (Bloomington stock, Df(3R)Ptp99A[R3]), (7) $ninaE^{I17}$ (null mutant flies lacking Rh1), and (8) eya^1 (flies lacking eyes). Nitrocellulose membranes were stained with Ponceau S to ensure that each lane contained the appropriate amount of protein. All lanes were loaded with protein extracts from two head samples of flies 0–3 days old, prior to retinal degeneration.

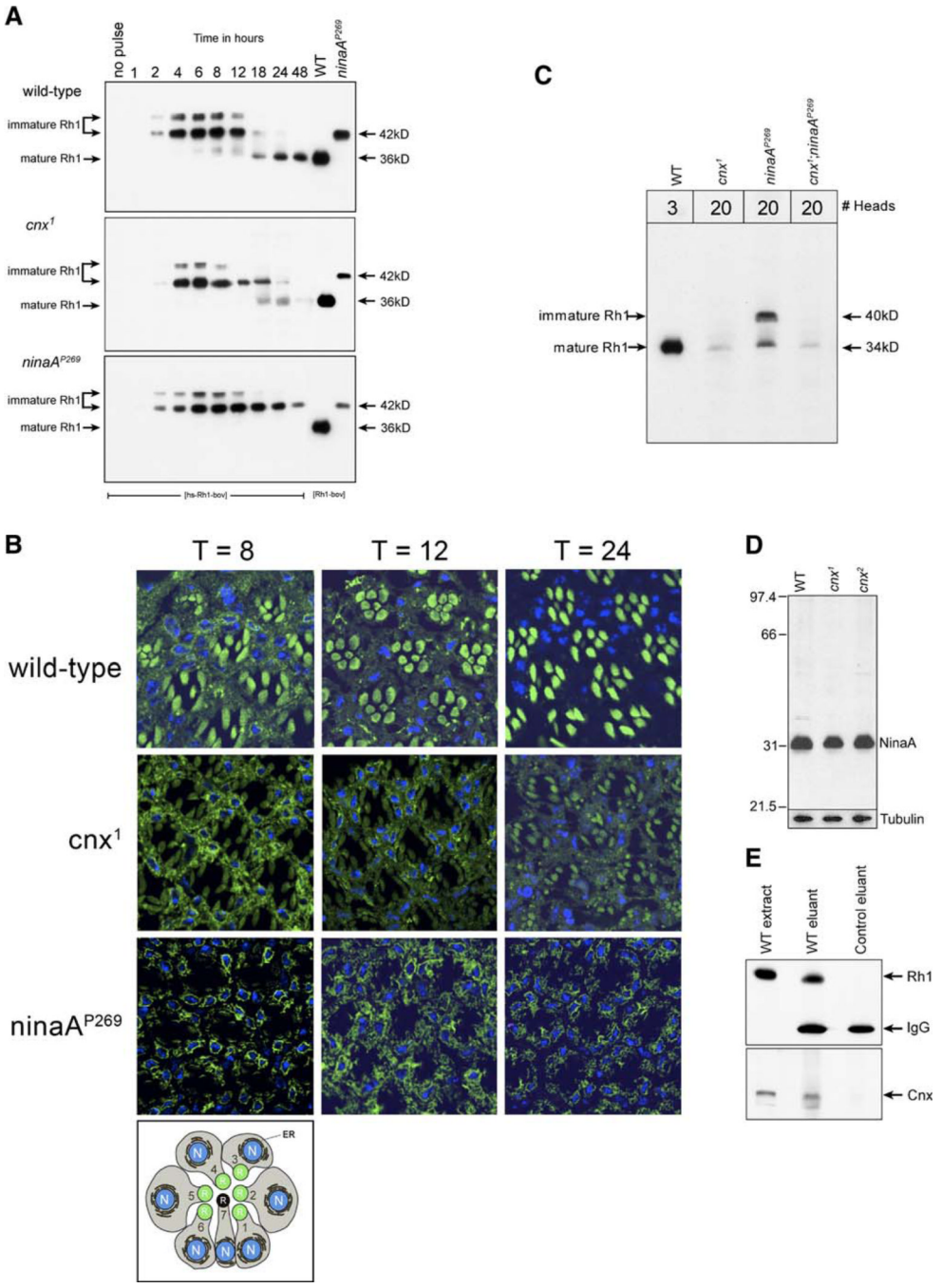

Figure 3. Calnexin Is Required by Rh1

(A) Cnx was required for effective Rh1 maturation and stability. Immunoblot of proteins isolated from heads of 0- to 2-day-old flies, prior to retinal degeneration were labeled with the 1D4 monoclonal antibody. Transgenic animals carrying the Rh1 gene under the control of a heat-shock promoter (hs) and tagged with the bov-epitope (*hs-Rh1-bov*) were given a 1 hr heat-pulse at 37°C and assayed at the indicated times after being shifted to 22°C. Numbers across the top refer to time in hours including both the hour of heat-pulse and the hours of chase. For example, lane 1 represents animals sampled prior to heat-pulse (no pulse), lane 2 represents animals sampled directly after the heat-pulse, and lane 3 represents animals given the 1 hr heat-pulse followed by a 1 hr chase. (Top) Wild-type (two heads per

lane), (middle) *cnx*^{1} (five heads per lane for lanes 1–7 and 20 heads per lane for lanes 8–10), (bottom) *ninaA*^{P269}, null allele (five heads per lane). In the *cnx* mutants, 20 heads were loaded per lane, at the later time points, to view the small amount of Rh1 that remained. For reference, lanes 11 and 12 show Rh1-bov expressed in wt and ninaA^{P269} flies, respectively (Rh1 promoter). The bov-epitope tag adds ~2 kDa to the MW of Rh1 such that the immature high-MW form is detected at 42 kDa and the mature low-MW form is 36 kDa. The nitrocellulose membranes were stained with 0.05% Ponceau S to ensure that each lane contained the appropriate amount of protein.

(B) Cnx is required for effective Rh1 maturation and stability. Transgenic animals were subjected to the same heat-pulse chase paradigm outlined in (A). Animals were fixed for immunocytochemistry at 8, 12, and 24 hr following the initiation of the heat-pulse. Confocal images of 0.5 μm thick cross-sections were immunolabeled with the 1D4 monoclonal antibody (green). Nuclei were stained with ToPro3 (blue). Numbers across the top refer to hours of chase following the initiation of the heat-pulse. (Top row) Wild-type, (middle row) *cnx*^{1}, (bottom row) *ninaA*^{P269}. The bottom panel is a schematic of a cross-section of the R1-7 photoreceptor cells. The rhabdomeres of the R1-6 photoreceptors are shown in green (R). The endoplasmic reticulum (ER, black) is shown around the nuclei (N, blue).

(C) Genetic interaction between *ninaA* and *cnx* mutants. Immunoblot of proteins isolated from heads of young flies prior to retinal degeneration were labeled with an antibody directed to Rh1 (4C5). (1) Wild-type (*bw;st*), (2) *cnx*^{1}, (3) *ninaA*^{P269}, (4) *cnx*^{1}/*ninaA*^{P269} double mutant. The nitrocellulose membranes were stained with 0.05% Ponceau S to ensure that each lane contained the appropriate amount of protein. Numbers at the top refer to number of fly heads loaded per lane.

(D) NinaA was expressed normally in the *cnx* mutants. (1) Wild-type (*bw;st*), (2) *cnx*^{1}, (3) *cnx*^{2}. Flies assayed in all of the lanes were 1–2 days old. The nitrocellulose membranes were stained with 0.05% Ponceau S to ensure that each lane contained the appropriate amount of protein. The same blot was reprobed with anti-tubulin antibody. Five heads were loaded per lane.

(E) Rh1 associates with the molecular chaperone Cnx. Rh1-Cnx complexes were isolated by immunoaffinity chromatography using the antibody directed to Rh1 (4C5 mouse monoclonal antibody). The bound fraction was eluted and subjected to SDS-PAGE and immunoblotting for (top) Rh1 protein (4C5 mouse monoclonal antibody) and (bottom) Cnx protein (rabbit polyclonal antibody). (1) Rh1 and Cnx are present in extracts from wt heads (Canton S). (2) Elution of bound fractions from wt fly extracts reveals that Rh1 binds to the immunoaffinity column (top) and Cnx coelutes with Rh1 (bottom). (3) Elution of bound fractions from *ninaE*^{I17} flies (flies carrying a deletion in the endogenous Rh1 gene) reveals that when Rh1 is not bound to the column (top), the Cnx protein is not detected in the eluant (bottom). Lanes containing the eluants (2 and 3) and probed for Rh1, reveal the IgG light chain of the 4C5 antibody, which is detected by the secondary antibody used in the immunoblot (top).

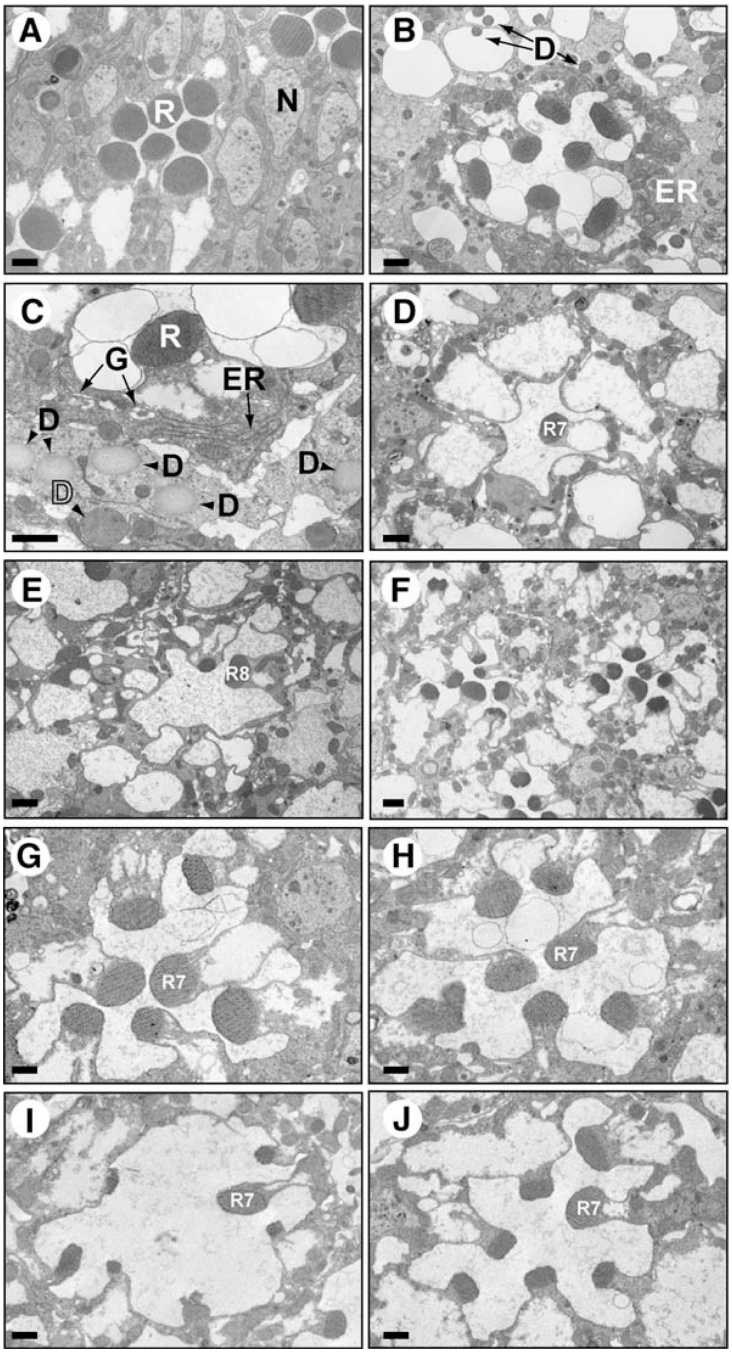

Figure 4. Cnx Mutants Displayed Age-Related Retinal Degeneration that Was Enhanced by Light

Electron micrographs of cross-sections through mutant and wt fly eyes. Flies were raised either on a 12:12 light-dark (L/D) cycle (A–E and G, I, J) or in constant darkness (F and H). Scale bars, 0.5 um. (A) Wild-type, (B) 1-day-old cnx^1 mutant, (C) a higher magnification of a 1-day-old cnx^1 mutant, (D) the apical portion of a 1-month-old cnx^1 mutant showing the R7 cell rhabdomere (R7). (E) The basal portion of a 1-month-old cnx^1 mutant showing the R8 cell rhabdomere (R8). (F) One-month-old cnx^1 mutant fly raised in constant darkness. (G) One-month-old $ninaA^{P269}$ mutant fly. (H) One-month-old $ninaA^{P269}$ mutant fly raised in constant darkness. (I) One-week-old cnx^1 mutant. (J) One-week-old $norpA^{P24};cnx^1$

double mutant, demonstrating that *norpA* confers protection from the light-dependent portion of the retinal degeneration. R, rhabdomere; N, nucleus; ER, endoplasmic reticulum; G, dilated Golgi; and D, deposits.

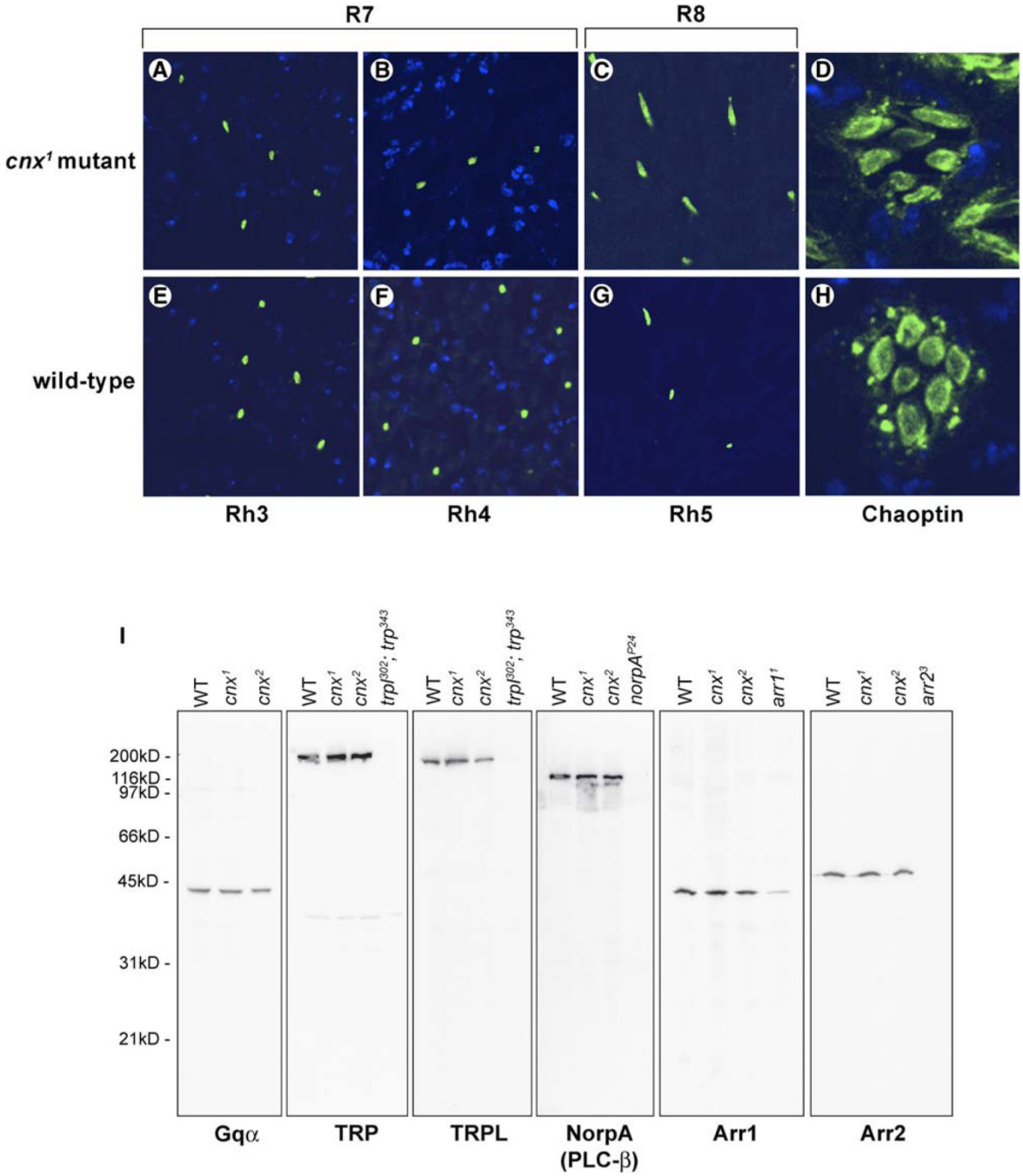

Figure 5. Calnexin Is Specifically Required by Rh1

(A–H) Cnx was not required for the expression of the R7 and R8 photoreceptor cell opsins: Rh3, Rh4, and Rh5. Shown here are confocal images of cross-sections through 1-day-old *cnx*^{1} mutant fly eyes (A–D) compared to wt (*bw;st*) (E–H) that were immunolabeled with monoclonal antibodies directed to either Rh3 (A and E), Rh4 (B and F), Rh5 (C and G) opsins, or chaoptin (D and H). In all eight micrographs, the rhabdomeres were labeled green (arrowheads). Nuclei were stained with ToPro3 (blue).

(I) Phototransduction proteins were expressed normally in *cnx* mutants. Shown here is a composite image of immunoblotting results for six photoreceptor cell proteins. They were all expressed at normal levels in both of the *cnx*^{1} and *cnx*^{2} mutant alleles. From left to right:

G protein α subunit (Gqα), transient receptor potential (TRP), and transient receptor potential-like (TRPL) channels, NorpA, which is PLCβ, arrestin 1 (Arr1), and arrestin 2 (Arr2) were all detected in wt (*bw;st*) and in both of the cnx^{1} and cnx^{2} mutant alleles. Flies assayed in all of the lanes were less than 4 days old. Mutant flies were used as controls for antibody specificity (from left to right): TRP and TRPL ($trpl^{302}$; trp^{343}), NorpA ($norpA^{P24}$, null allele), Arr1 ($arr1^{1}$, expresses 10% of wt levels of Arr1 [Dolph et al., 1993]), and Arr2 ($arr2^{3}$). The nitrocellulose membranes were stained with 0.05% Ponceau S to ensure that each lane contained the appropriate amount of protein. Five heads were loaded per lane.

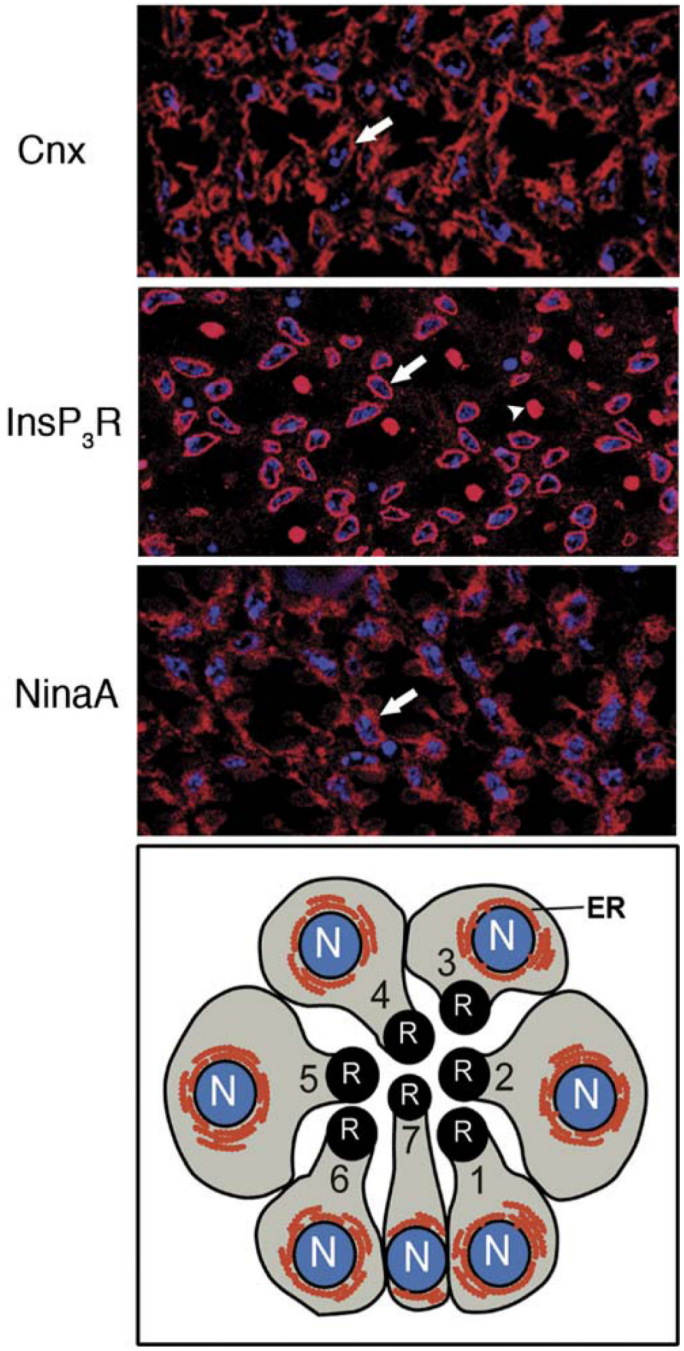

Figure 6. Cnx Is Expressed in the ER of All Eight Photoreceptor Cells

Confocal images of cross-sections from wt eyes immunolabeled with polyclonal rabbit antibodies directed to (top) Cnx, (middle) $InsP_3R$, and (bottom) NinaA. Nuclei were stained with ToPro3 (blue). (Arrows) Perinuclear labeling; (arrowhead) nonspecific labeling of R7 rhabdomere with the $InsP_3R$ antibody. (Below) A schematic of a cross-section from the R1-7 photoreceptor cells. The rhabdomere (R) is the photosensitive organelle comprised of numerous microvili containing the rhodopsin photopigments and the other components of the phototransduction cascade. The endoplasmic reticular (ER) membrane system (red)is extensive in the photoreceptor cells and is perinuclear as well as elsewhere in the photoreceptor cells, nuclei (N, blue).

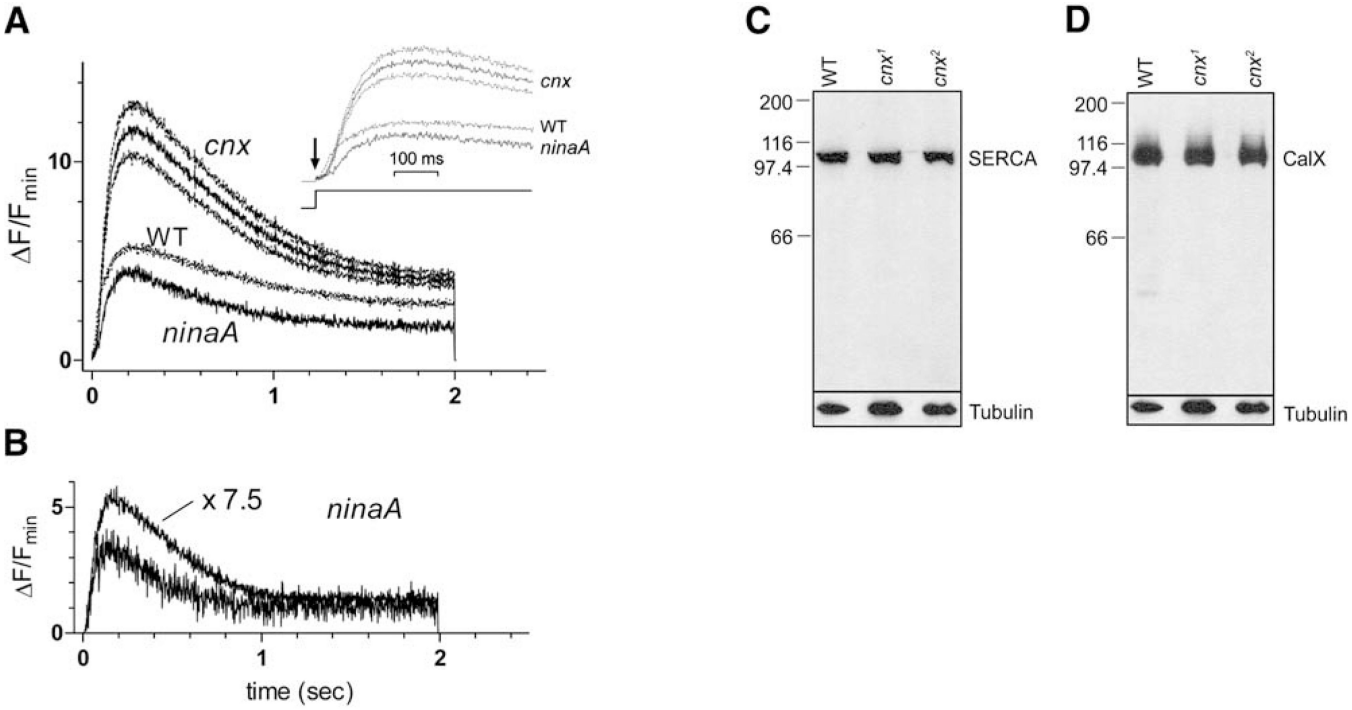

Figure 7. Ca^{2+} Measurements in *cnx*, WT, and *ninaA*

(A) Ca^{2+} indicator measurements in *cnx*, wt, and $ninaA^{P269}$ photoreceptors loaded with the low-affinity single-wavelength indicator dye Fluo-4FF (100 μM) via the patch pipette and illuminated for 2 s with the same intensity 485 nm light (equivalent to ~10^8 effectively absorbed photons/s in wt flies). Traces show the mean from n = 15cnx (cnx^1 and cnx^2 pooled), 10 wt, and 7 *ninaA* cells. For clarity, the error range(±SEM) is shown only for *cnx*. (B) In a $ninaA^{P269}$ cell, a second much brighter stimulus (7.5-fold higher intensity) induced only a slightly greater Ca^{2+} rise, excluding the possibility that the slightly greater quantum catch in *cnx* mutants (Figure S2) could underlie the greatly increased Ca^{2+} signal in the *cnx* mutants (n = 3). (C) SERCA and (D) CalX were expressed normally in the *cnx* mutants. (1) Wild-type (*bw;st*), (2) cnx^1, (3) cnx^2. Flies assayed in all of the lanes were 1–2 days old. The nitrocellulose membranes were stained with 0.05% Ponceau S to ensure that each lane contained the appropriate amount of protein. The same blot was reprobed with anti-tubulin antibody. Five heads were loaded per lane.